Electrochemical design of plasmonic nanoantennas for tip-enhanced optical spectroscopy and imaging performance

Sergey Kharintsev,[1,*] Alexander Alekseev,[2] Valeria Vasilchenko,[1] Anton Kharitonov,[1] and Myakzyum Salakhov[1]

[1]*Department of Optics and Nanophotonics, Institute of Physics, Kazan Federal University, Kremlevskaya str., 16, Kazan, Tatarstan, 420008, Russia*

[2]*National Laboratory Astana, Nazarbayev University, Kabanbay Batyr Ave., 53, Astana, 01000, Kazakhstan*

[*]*skharint@gmail.com*

Abstract: Optical nanoantennas play a crucial role in controlling near-fields on the nanoscale and being counterparts of commonly used conventional optical components such as lens, prisms, gratings, etc. for shaping the wavefront of light in the far-field. In this paper we highlight a dc-pulsed voltage electrochemical etching method with a self-tuneable duty cycle for highly reproducible design of plasmonic (metallic) nanoantennas. With the method, we introduce such concepts as design, optimization and figure-of-merit for evaluating fabrication efficiency. The ability of the nanoantennas to enhance and localize the optical fields beyond the diffraction limit is statistically studied with Rayleigh scattering from the tip apex and tip-enhanced Raman spectroscopy of a single walled carbon nanotubes bundle.

OCIS codes: (240.0240) Optics at surfaces; (240.6695) Surface-enhanced Raman scattering; (250.5403) Plasmonics.

References and links

1. L. Novotny and B. Hecht, *Principle of Nano-Optics* (Cambridge University Press, 2012).
2. P. Verma, T. Ichimura, T. Yano, Y. Saito, and S. Kawata, "Nano-imaging through tip-enhanced Raman spectroscopy: Stepping beyond the classical limits," Laser Photonics Rev. **4**(4), 548–561 (2010).
3. A. Zayats and S. Maier, *Active Plasmonics and Tuneable Plasmonic Metamaterials* (John Wiley & Sons, 2013).
4. M. Agio and A. Alu, *Optical Antennas* (Cambridge University Press, 2013).
5. L. Novotny, "From near-field optics to optical antennas," Phys. Today **64**(7), 47–52 (2011).
6. P. Bharadwaj, B. Deutsch, and L. Novotny, "Optical antennas," Adv. Opt. Photonics **1**(3), 438 (2009).
7. A. Bouhelier, R. Bachelot, G. Lerondel, S. Kostcheev, P. Royer, and G. P. Wiederrecht, "Surface Plasmon Characteristics of Tunable Photoluminescence in Single Gold Nanorods," Phys. Rev. Lett. **95**(26), 267405 (2005).
8. C. Höppener, Z. J. Lapin, P. Bharadwaj, and L. Novotny, "Self-Similar Gold-Nanoparticle Antennas for a Cascaded Enhancement of the Optical Field," Phys. Rev. Lett. **109**(1), 017402 (2012).
9. T. Feichtner, O. Selig, M. Kiunke, and B. Hecht, "Evolutionary Optimization of Optical Antennas," Phys. Rev. Lett. **109**(12), 127701 (2012).
10. A. E. Krasnok, I. S. Maksymov, A. I. Denisyuk, P. A. Belov, A. E. Miroshnichenko, C. R. Simovskii, and Y. S. Kivshar, "Optical nanoantennas," Usp. Fiziol. Nauk **183**(6), 561–589 (2013).
11. B. Ren, G. Picardi, and B. Pettinger, "Preparation of gold tips suitable for tip-enhanced Raman spectroscopy and light emission by electrochemical etching," Rev. Sci. Instrum. **75**(4), 837 (2004).
12. X. Wang, Z. Liu, M.-D. Zhuang, H.-M. Zhang, X. Wang, Z.-X. Xie, D.-Y. Wu, B. Ren, and Z.-Q. Tian, "Tip-enhanced Raman spectroscopy for investigating adsorbed species on a single-crystal surface using electrochemically prepared Au tips," Appl. Phys. Lett. **91**(10), 101105 (2007).
13. L. Billot, L. Berguiga, M.L. de la Chapellea, Y. Gilbert, and R. Bachelot, "Production of gold tips for tip-enhanced near-field optical microscopy and spectroscopy: analysis of the etching parameters," J. Appl. Phys. **31**, 139–145 (2005).
14. L. Jiang-Tao, Y. Yan, W.-K. Zhang, Y.-H. Liu, Z.-Y. Jiang, and G.-Y. Si, "Plasmonic nanoantennae fabricated by focused Ion beam milling," Int. J. Precis. Eng. Manuf. **16**(4), 851–855 (2015).
15. C. Ropers, C. C. Neacsu, T. Elsaesser, M. Albrecht, M. B. Raschke, and C. Lienau, "Grating-coupling of surface plasmons onto metallic tips: a nanoconfined light source," Nano Lett. **7**(9), 2784–2788 (2007).
16. I. Maouli, A. Taguchi, Y. Saito, S. Kawata, and P. Verma, "Optical antennas for tunable enhancement in tip-enhansed Raman spectroscopy imaging," Appl. Phys. Express **8**(3), 032401 (2015).

#245964 Received 14 Jul 2015; revised 2 Sep 2015; accepted 8 Sep 2015; published 15 Sep 2015

17. O. Tanirah, D. P. Kern, and M. Fleischer, "Fabrication of a plasmonic nanocone on top of an AFM cantilever," Microelectron. Eng. **141**, 215–218 (2015).
18. R. Zhang, Y. Zhang, Z. C. Dong, S. Jiang, C. Zhang, L. G. Chen, L. Zhang, Y. Liao, J. Aizpurua, Y. Luo, J. L. Yang, and J. G. Hou, "Chemical mapping of a single molecule by plasmon-enhanced Raman scattering," Nature **498**(7452), 82–86 (2013).
19. J. Stadler, B. Oswald, T. Schmid, and R. Zenobi, "Characterizing unusual metal substrates for gap-mode tip-enhanced Raman spectroscopy," J. Raman Spectrosc. **44**(2), 227–233 (2013).
20. J. Stadler, T. Schmid, and R. Zenobi, "Nanoscale chemical imaging using top-illumination tip-enhanced Raman spectroscopy," Nano Lett. **10**(11), 4514–4520 (2010).
21. S. S. Kharintsev, A. I. Noskov, G. G. Hoffmann, and J. Loos, "Near-field optical taper antennas fabricated with a highly replicable ac electrochemical etching method," Nanotechnology **22**(2), 025202 (2011).
22. S. S. Kharintsev, G. G. Hoffmann, A. I. Fishman, and M. K. Salakhov, "Plasmonic optical antenna design for performing tip-enhanced Raman spectroscopy and microscopy," J. Phys. D Appl. Phys. **46**(14), 145501 (2013).
23. T. Ward, "Electrohydrostatic wetting of poorly-conducting liquids," J. Electrost. **64**(12), 817–825 (2006).
24. S. S. Kharintsev, A. M. Rogov, and S. G. Kazarian, "Nanopatterning and tuning of optical taper antenna apex for tip-enhanced Raman scattering performance," Rev. Sci. Instrum. **84**(9), 093106 (2013).

1. Introduction

Unlike the diffraction-limited optical elements operated as low frequency filters, plasmonic (metallic) nanoantennas, being nanoscale optical devices for converting near-to-far-fields and back, provide an access not only to high spatial frequencies but imaginary ones as well [1]. It means that the plasmonic nanoantennas handle both propagating and non-propagating (confined) optical fields and, thus, they assist to gain an insight into inherent mechanisms of light-matter interactions at the nanometric scale. This ability gives a stimulus for developing enhanced spectroscopy and near-field imaging [2] and, most importantly, opens the door for active plasmonics and integrated optoelectronics [3].

Design and optimization of optical antennas have become one of the most exciting and rapidly developing research area of enhanced optical microscopy in the last few years [4]. The underlying photon-electron excitation mechanism, often referred to as a surface plasmon-polariton, in confined metallic nanostructures provides a strong light confinement and leads to high ohmic loss. The latter is a crucial factor for waveguide purposes only and, therefore, being out of our study. Under design of the optical antennas, the morphology of their mesoscopic surface is commonly understood; in particular, one deals with nanoparticles, nanorods, conical tips, self-similar antennas, bow-tie gap antennas, tip-on-aperture antennas and others [5–9]. A complete list of optical antennas designs can be found in the following sound review [10]. In most cases, electrochemical etching [11–13] and focused ion beam milling [14] are utilized for fabricating the optical antennas. With the methods, a considerable progress has been achieved for mainly shaping mesoscopic surfaces of the optical antennas [15], whereas the reproducibility and reliability of a well-controlled hot spot tip or gap geometry are still painful. In our opinion, this is one of possible reasons why an interest to tip-enhanced Raman scattering (TERS) performance with bulk plasmonic gold/silver tips operating in tapping mode becomes depressed. To date, most TERS experiments are performed with gold/silver deposited atomic force microscopy (AFM) [16,17] or scanning tunneling microscopy (STM) probe [18]. For reinforcing the light confinement between the tip apex operating in tapping mode and a specimen of interest, a substrate is often deposited with a plasmonic material for exciting gap modes [19,20].

Electrochemical etching is widely used as a low-cost, simple and reliable fabrication tool for designing plasmonic optical conical nanoantennas with a high yield of >90% [21,22]. A drawback of this method is related to optimization of a large number of parameters such as the chemical nature of etching electrolyte, electrode arrangement, an applied voltage shape, etching timing, a cutoff current and others.

In this paper, we develop a dc-pulsed voltage electrochemical etching method with a self-tuneable duty cycle for highly reproducible design of plasmonic nanoantennas. Bent gold tips are attached to tuning fork sensors for performing TERS measurements with top-illumination configuration in tapping mode in air, as shown Fig. 1(a). This method allows one to give a new interpretation for design and optimization of optical antennas. A figure-of-merit is introduced for statistically evaluating fabrication efficiency. A TERS-activity of the antennas

#245964 Received 14 Jul 2015; revised 2 Sep 2015; accepted 8 Sep 2015; published 15 Sep 2015

is probed with a plasmon-enhanced frequency-shifted optical response from a single walled carbon nanotubes bundle.

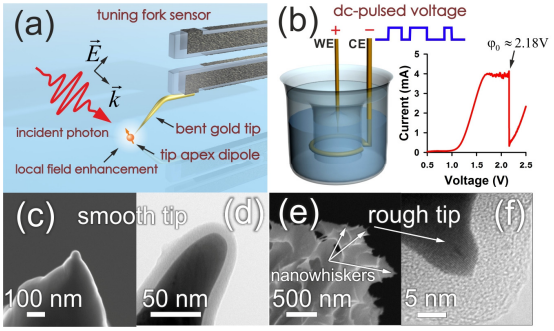

Fig. 1. Sketch of an incident photon and gold tip coupling (a), two-electrode chemical cell and linear sweep voltammetry for gold wire in a mixture of HCl and Ethanol (1:1) (b), SEM images of smooth (c) and rough (e) tips and TEM images of their tip apexes (d) and (f), respectively.

2. DC-pulsed voltage etching with self-tuneable duty cycle

In our method we use a two-electrode chemical cell with an inner bottom-free beaker (Fig. 1(b)), in which a voltage square wave is applied between a working electrode (WE), which is a 100μm gold wire (purity: 99.99%, GoodFellow, UK), and a gold ring counter electrode (CE). Without loss of generality we use a solution of fuming hydrochloric acid (HCl, 37%) and ethanol (C_2H_5OH, 96%) in a volume proportion of 1: 1 as an etching electrolyte [11–13]. Figure 1(b) shows a linear sweep voltammetry analysis of a 100 μm gold wire in the etchant. At a voltage of 2.18 V we observe an abrupt drop in etching current because of passivation of WE with chloroaurate complexes $AuCl_{4-x}[OH]^-$ [11,22] which block an access for Cl^- anions to WE in the vicinity of an etchant meniscus. This value corresponds to an electrode potential of 1.68 V for gold at which a leading corrosion mechanism $Au \leftrightarrow Au^+ + e^-$ takes place [21].

Importantly, electrochemical etching is generally non-steady, since convex areas on the gold surface dissolve strongly in comparison with concave ones and, in addition, the gold under stress corrodes faster than that in a normal state. Thus, a choice of a voltage shape plays a key role in producing gold tips. The simplest designs can be performed by varying a dc voltage value, for example, a sharp smooth tip (Fig. 1(c), 1(d)) and a highly rough tip (Fig. 1(e), 1(f)) come into reality at 2 V and 1.5 V, respectively, in a reproducible way. The rough tip contains numerous nano-tips and nano-edges on its top, each of that can be potentially used as a plasmonic antenna. In order to make this process robust, a controllable mechanical mixing is needed. For this purpose, it is often used a square wave voltage with top and bottom values of V_t and V_b. The height-of-rise of the meniscus $\Delta h(t)$ is driven as $\Delta h(t) \sim |V_t - V_b| = \Delta V$ provided that $\Delta V \ll (V_t + V_b)/2$. This originates from the capacitance model or the Maxwell stress tensor in the case of a non-charged interfacial surface [23]. Thus, one of the ways to overcome blocking corrosion because of the passivation layer is the dc-pulsed voltage etching method [22]. With this, a voltage-driven meniscus performs oscillations along the gold wire and, therefore, mechanical mixing of the solution near the interface takes place. In other words, upward/downward motion of the meniscus speeds up the diffusion of corrosion products. It has been found [22,24] that the etching current kinetics is followed by the fractional Brownian motion model and satisfies a power law with a complex fractional exponent, namely, $I(t) \sim t^{\alpha+i\beta}$ (where the fractional exponent α describes a transport of chlorides through a barrier layer (diffusion) and the imaginary part β corresponds to losses of Cl^- because of oxidation).

#245964 Received 14 Jul 2015; revised 2 Sep 2015; accepted 8 Sep 2015; published 15 Sep 2015

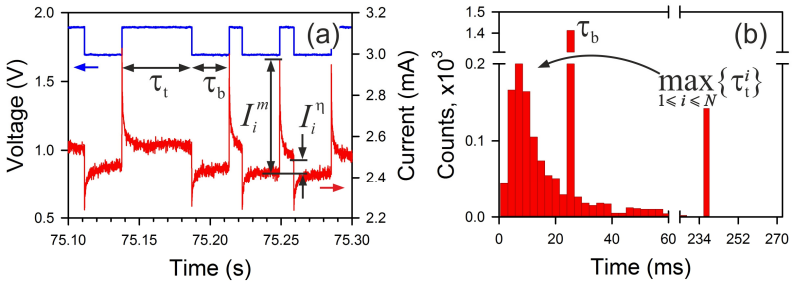

Fig. 2. DC-pulsed voltage etching with a self-tuneable duty cycle (voltage and current curves) (a), a histogram of impulse lengths (b).

A self-similar behaviour of the etching current during the etching allows us to introduce a handling parameter η as a ratio of a current value I_i^{η} and a maximal current I_i^m in the i-th impulse (Fig. 2(a)) at a top voltage value of V_t. As follows from this figure, the etching current relaxes towards a plateau because of sluggish downward motion of the meniscus. Generally, the impulse lengths τ_t and τ_b (or the duty cycle, defined as $D = \tau_t/(\tau_t + \tau_b)$) should be empirically found for the dc-pulsed voltage etching method. However, this is a rather difficult task, since the relaxation time decreases with thinning of the gold wire, that is, when its radius tends to zero. With the reason, etching current fluctuations strongly increase and it ultimately influences the tip apex shaping. To avoid undesirable over-etching and under-etching effects at a final stage the impulse length τ_t at V_t should be correlated with the relaxation time of the etching current. In our experiment τ_t is driven by itself due to the parameter η, which is within a range of 10-20%. The impulse length τ_b at a bottom voltage value of V_b is fixed and equals a 10% value of the impulse period $T = \tau_t + \tau_b$. Figure 2(b) shows a histogram of impulse lengths with the self-tuneable duty cycle. The impulse length τ_b and period T are equaled to 26.2 ms and 262 ms, respectively. We observe a redistribution of the impulse lengths $\{\tau_t^i\}$ ($i = 1,\ldots,N$), which are limited to 236 ms, with a centre of gravity of ~8 ms. The latter for different gold tips ranges statistically from 2 ms to 20 ms and it means that a time sampling when etching is estimated to be ~100 μs. Such a time is enough to meet a current cutoff event in an optimal manner [21,24]. The centre of gravity of the histogram is long-term shifted when the handling parameter η increases and vice versa. If the latter tends to zero then a log-normal distribution of the impulse lengths τ_t is converted into an exponential one. Closing this section we conclude that self-adjustment of the time length τ_t may benefit for highly replicable electrochemical etching TERS active gold tips.

3. Design and optimization of gold conical antennas

Previously, the reproducibility of gold tips etched with the method had been determined as a probability to find tips with curvature radii ρ falling in the range of interest [21]. However, this approach may distort the yield of the well-shaped tips produced with the dc-voltage etching method because of non-uniform distribution. We have prepared 10 gold tips with both the dc-etching method (Fig. 3(a)) and adaptive etching method (Fig. 3(b)) for evaluating their power. Scanning electron images of the tip apexes are given in the insets. The histograms are well fitted to a lognormal distribution. As follows from Fig. 3(b), the uncertainty $\Delta\rho$ noticeably squeezes for etching with the self-tuneable duty cycle. This finding provides an evidence for a controllable motion of the electrolyte meniscus and, therefore, adaptive etching. With the latter, we may interpretate design and optimization as handling an average

#245964 Received 14 Jul 2015; revised 2 Sep 2015; accepted 8 Sep 2015; published 15 Sep 2015

value $\bar{\rho}$ and uncertainty $\Delta\rho$. In this context we deal with the design of the tip apexes rather than the morphology of the mesoscopic surface. By varying the surface tension of the etchant, the average value $\bar{\rho}$ can be adjusted. This makes the adaptive etching a powerful tool for designing TERS active gold tips. To quantitatively characterize the power of this method, a figure-of-merit can be defined as $f = \bar{\rho}/\Delta\rho$. This criterion is not suitable for the dc- or dc-pulsed voltage etching methods because $\bar{\rho} \ll \Delta\rho$. The reproducibility of the tip apexes with the curvature radii $\bar{\rho}_1$ and $\bar{\rho}_2$ (for example, $\bar{\rho}_1 > \bar{\rho}_2$) implies that their uncertainties $\Delta\rho_1$ and $\Delta\rho_2$ satisfy an inequality $\Delta\rho_1 < \Delta\rho_2$. In others words, there is, in a statistical sense, a lower limit for the gold tips fabricated with the electrochemical etching methods.

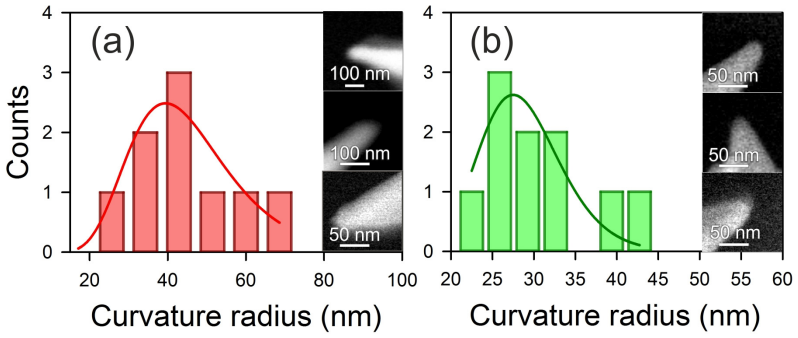

Fig. 3. A histogram of curvature radii of gold tips fabricated with dc-etching (1) and adaptive etching (2).

Probing a TERS activity of the gold tips is one of important steps in their design and optimization. Under TERS-active tips we understand optical antennas capable to enhance and localize a laser light due to the plasmonic effect. For this purpose, a hybrid scanning probe microscope equipped with an optical spectrometer NTEGRA SPECTRA (NT-MDT, Russia) has been utilized. For a statistical analysis, we prepared 20 gold tips with both the dc-etching method and the adaptive method. They were glued to a tuning fork that oscillates at a resonance frequency of ~32 kHz, as shown in Fig. 1(a). In the upright optical scheme, a weakly focused laser beam is used for probing hot spots of the bent gold tip with longitudinal and transverse modes of the electric field. This is easily reached with a x100 objective with a high numerical aperture of 0.7. For testing a plasmonic effect and evaluating the field enhancement, we used a single-walled carbon nanotubes bundle (HiPCo, Carbon Nanotechnology Inc.) as a proper one-dimensional object with strong Raman-active spectral lines. Among them the peaks at 1575 cm^{-1} and 1592 cm^{-1} assigned to $G^-(E_{1g})$ and $G^+(A_{1g})$ modes, respectively, are often exploited. Figure 4(a) demonstrates a histogram of the field enhancement, defined as a ratio of near-field (tip on) and far-field (tip off) intensities (see the inset). We see that only half of all tips turns out to be plasmonic. Certainly, this yield is critically dependent on the orientation of the tip apex in respect to a polarization of the incident laser light. The plasmonic effect occurs for a upright tip affected with the longitudinal excitation. Because of the tip inclination effect the tip-light coupling becomes depressed [24].

An alternative way to probe the plasmonic activity of the gold tip is related to Rayleigh scattering from the tip apex which is raster scanned over a laser spot. A two-lobe pattern occurs when the upright tip is illuminated with a highly focused linearly polarized light and this optical fingerprint is not dependent on the polarization direction. In a case of the bent gold tip (Fig. 1(a)) the two-lobe optical response comes into reality when the tip axis coincides with the E_x-polarization (Fig. 4(b)), otherwise no lobes at the rims of the focal spot appear when the E_y-polarization is used (Fig. 4(c)). Unambiguous recognition of the

#245964 Received 14 Jul 2015; revised 2 Sep 2015; accepted 8 Sep 2015; published 15 Sep 2015

plasmonic activity is feasible with an azimuthally-polarized doughnut laser light. The axially symmetric transverse mode couples with the bent tip irrespective of its tilt. However, this mode becomes “blind” for the upright tip. A highly focused radially-polarized light with the blended polarization, due to longitudinal and transverse contributions, holds a promise for evaluating the plasmonic activity of the gold tips.

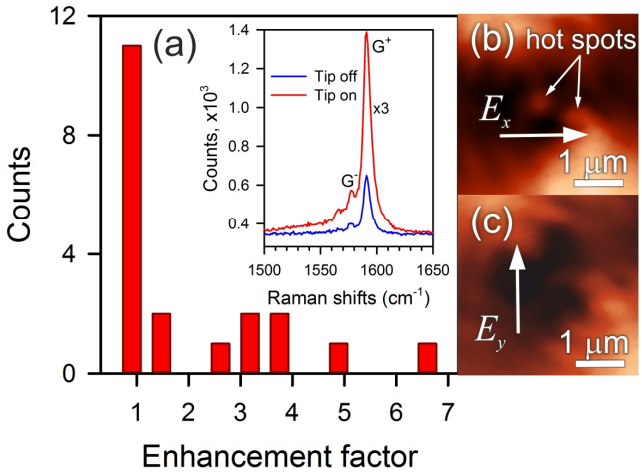

Fig. 4. A histogram of the field-enhancement factor (a), optical patterns of tips illuminated with a linearly polarized light (b) and (c).

4. Conclusion

In this paper we developed a dc-pulsed voltage electrochemical etching method with a self-tuneable duty cycle for highly reproducible design of smooth gold tips. The underlying mechanism is related to controlling etching current kinetics through an *in situ* analysis of relaxation times under a voltage attack. It has been revealed that adaptive etching narrows a range of curvature radii of tip apexes falling within a confidential interval. In a context of the method, under the optical nanoantenna design we understand a controlled fabrication of gold tips with the average curvature radius of the tip apexes $\bar{\rho}$ provided that $\bar{\rho} \gg \Delta\rho$. In other words, the figure-of-merit of the method essentially exceeds unity, that is, $f = \bar{\rho}/\Delta\rho \gg 1$. It means that optimization of the etching method is aimed at minimization of the uncertainty $\Delta\rho$. A suitability of the gold tips to control optical near-fields was statistically analyzed with a plasmon-enhanced Raman spectroscopy of a single walled carbon nanotubes bundle. An alternative indicator of the plasmonic effect is rotation of a two-lobe Rayleigh scattering pattern coming from the upright gold tip illuminated with a highly focused linearly-polarized light. In the case of bent gold tips the same effect is observed when the azimuthally polarized light is used.

Acknowledgments

This work was financially supported by the Russian Foundation for Basic Research (No. 15-42-02339). Work of A.A. was supported by Nazarbayev University-Lowrence Berkeley Nation Laboratory cooperation program, grant #4. The authors are indebted to Prof. A.I. Fishman (Kazan Federal University) for his help in preparing the paper. This work was done using equipment of Federal Center of Shared Equipment of Kazan Federal University.

#245964 Received 14 Jul 2015; revised 2 Sep 2015; accepted 8 Sep 2015; published 15 Sep 2015